THIS MONTH IN

JNM

Updated SSR imaging guideline: Balon offers background and perspective on the revised version of the SNM Practice Guideline for Somatostatin Receptor Scintigraphy that appears this month in the *Journal of Nuclear Medicine Technology*. . . . . ***Page 1838***

Toward clinical Raman spectroscopy: Zavaleta and colleagues provide an overview of the development and applications of this novel optical technology in molecular imaging, from in vitro studies to preclinical, clinical, and future capabilities. . . . ***Page 1839***

Reassessing pediatric imaging: Zanzonico offers perspective on elements involved in balancing the benefits of advanced imaging techniques against risks of radiation exposure in young patients and previews a related article in this issue of *JNM*. . . . ***Page 1845***

Plaque imaging with ^{11}C-acetate: Derlin and colleagues examine the distribution and topographic relationship of ^{11}C-acetate uptake and vascular calcification in major arteries in preparation for PET/CT imaging of fatty acid synthesis in atherosclerotic vessel walls . . . . . ***Page 1848***

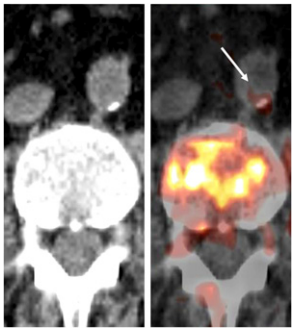

PET/CT in thyroid cancer: Kauhanen and colleagues compare the abilities of ^{18}F-DOPA and ^{18}F-FDG PET/CT with those of MRI in localization of metastatic disease in recurrent or persistent medullary thyroid cancer . . . . . ***Page 1855***

^{68}Ga-DOTATATE vs. ^{68}Ga-DOTATOC: Poeppel and colleagues evaluate the comparative utility of PET lesion detection with these radiolabeled somatostatin analogs in the same group of patients with neuroendocrine tumors . . . . . ***Page 1864***

^{18}F-FDG and ^{18}F-FLT PET in lung cancer: Kahraman and colleagues explore the prediction of clinical benefit from first-line erlotinib treatment using different quantitative parameters for both ^{18}F-FDG and ^{18}F-fluorothymidine PET in advanced non–small cell lung cancer. . . ***Page 1871***

Antibody–antigen relationships for huA33: O'Donoghue and colleagues use PET to analyze the quantitative features of antibody–antigen interactions in tumors and normal tissue after administration of ^{124}I-labeled antitumor antibodies to patients with colorectal cancer . . . . . ***Page 1878***

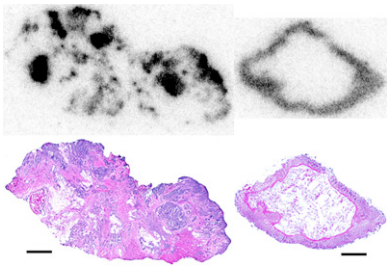

sst_2 antagonist vs. agonist binding: Cescato and colleagues assess in vitro binding of the ^{177}Lu-DOTA-Bass somatostatin receptor antagonist and the ^{177}Lu-DOTA-TATE agonist to a range of sst_2-expressing human tumor samples . . . . . ***Page 1886***

Arm motion and PET/CT: Lodge and colleagues investigate the mechanisms that underlie arm motion–induced cold artifacts on whole-body PET/CT images and propose a potential solution . . . . ***Page 1891***

^{18}F-FLT PET in MCL: Herrmann and colleagues report on the ability of this in vivo proliferation marker to characterize mantle cell lymphoma and discuss its promise in clinical management . . . . . ***Page 1898***

Imaging in sarcoma: Eary and Conrad offer an educational overview of ^{18}F-FDG PET in sarcoma diagnosis and treatment response and highlight new areas of biologically specific PET techniques with potential for outcome stratification . . . . . ***Page 1903***

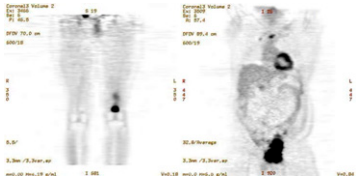

Biograph mMR performance: Delso and colleagues assess the performance of a new integrated whole-body PET/MR scanner during independent and simultaneous acquisition of PET and MR data. . . . . ***Page 1914***

Risk and benefit in pediatric imaging: Sgouros and colleagues describe a rigorous and critical approach to balancing the benefits of adequate image quality against radiation risks in children, using an example based in ^{99m}Tc-DMSA scanning . . . . ***Page 1923***

Fast 3D dosimetry for ^{90}Y-microspheres: Dieudonné and colleagues develop and evaluate a novel approach to standardized prescribed activity calculation in selective internal radiation therapy and highlight the potential value of 3D treatment planning strategies . . . . . ***Page 1930***

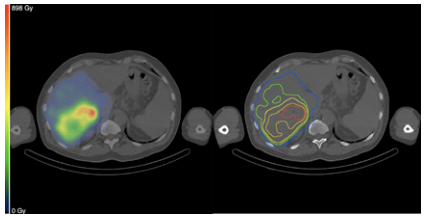

Radionuclide therapy in ovarian cancer: Zacchetti and colleagues assess the preclinical specificity of a ^{131}I-labeled human antibody fragment that binds to folate

receptors in ovary cancer cells and investigate its therapeutic efficacy in tumor models. . . . . ***Page 1938***

PET imaging of glutaminolysis: Lieberman and colleagues report on both in vitro and in vivo animal studies with ^{18}F-(2*S*,4*R*) 4-fluoroglutamine and detail its potential use as an alternative PET tracer for mapping glutaminolytic tumors . . ***Page 1947***

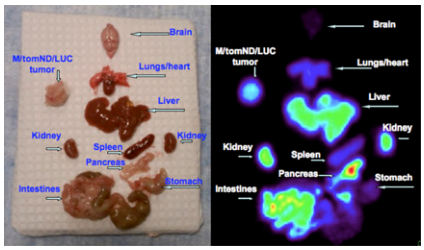

Imaging angiogenesis: Liu and colleagues detail the development of a novel ^{64}Cu-labeled nanoprobe that detects upregulation of natriuretic peptide clearance receptors and offers sensitive detection with PET during development of angiogenesis in a mouse model . . . ***Page 1956***

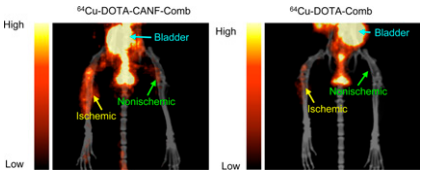

PET and gastric aromatase: Ozawa and colleagues use ^{11}C-vorozole PET to investigate gastric aromatase expression, which has been implicated in pathophysiologic states in various diseases via estrogen expression . . . . . ***Page 1964***

Bombesin antagonist for prostate imaging: Abiraj and colleagues detail the development of clinically translatable bombesin antagonist–based radioligands for SPECT and PET of gastrin-releasing peptide receptor–positive tumors . . . . . ***Page 1970***

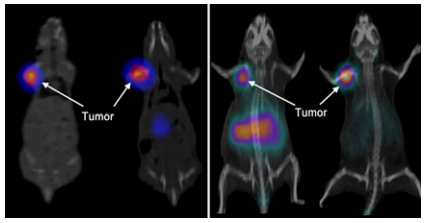

Cell-penetrating integrin $\alpha_2\beta_1$ probe: Huang and colleagues report on studies designed to improve the targeting efficacy of the DGEA peptide for near-infrared fluorescence and microPET imaging of integrin $\alpha_2\beta_1$ expression in prostate cancers . . . . ***Page 1979***

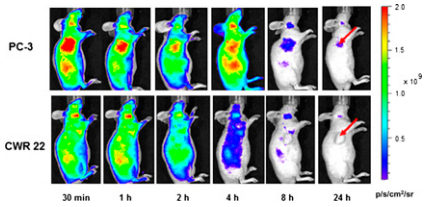

Semiquantitative stroke imaging in rats: Ceulemans and colleagues validate the use of ^{99m}Tc-HMPAO micro-SPECT/CT for semiquantification of infarct size after experimental stroke in rats. . . ***Page 1987***

Development, sex, and cardiac risk: Guiducci and colleagues explore in minipigs the lifetime influence of innate factors, including mother's metabolism and sex of offspring, on cardiometabolic risk, including organ-specific insulin resistance, subclinical cardiac dysfunction, and DNA oxidative damage . . . . . ***Page 1993***

^{89}Zr-fresolimumab PET: Oude Munnink and colleagues use radiolabeled fresolimumab, which neutralizes all mammalian forms of transforming growth factor-β, to analyze the growth factor's expression, antibody tumor uptake, and organ distribution in hamster models of human breast cancer . . . . . ***Page 2001***

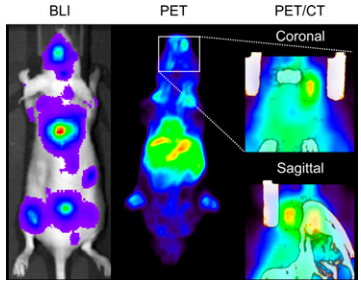

Advances in Cerenkov techniques: Xu and colleagues review the physics, cross-validations, and wide range of potential applications of Cerenkov luminescence imaging and highlight recent technical advances . . . . . ***Page 2009***

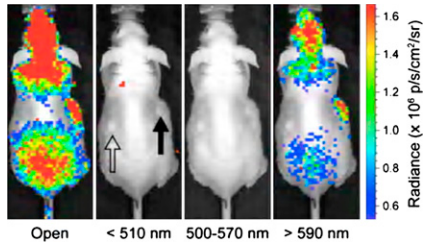

ON THE COVER

The recently released Biograph mMR is the first commercially available integrated whole-body PET/MR scanner. It has been shown to compare favorably with other state-of-the-art PET/CT and PET/MR scanners, indicating that the integration of the PET detectors in the MR scanner and their operation within the magnetic field do not have a perceptible impact on overall performance.

See page 1921.